Hydrogelation

DOI: 10.1002/anie.200703785

Structure Calculation of an Elastic Hydrogel from Sonication of Rigid Small Molecule Components**

*Kirsty M. Anderson, Graeme M. Day, Martin J. Paterson, Peter Byrne, Nigel Clarke, and Jonathan W. Steed**

The formation of hydrogels by the noncovalent assembly of organic molecules into nanoscale, cross-linked fibrous aggregates is highly topical and has been recently reviewed.[1] Hydrogels have wide-ranging potential applications in tissue engineering,[2,3] as vehicles for controlled drug delivery,[4,5] in the templated synthesis of nanoparticles and inorganic nanostructures,[6,7] in template polymerization,[8] and in pollutant capture and removal.[9] Small molecule hydrogelators frequently aggregate by hydrogen bonding, π-stacking, metal coordination,[8,10,11] and hydrophobic interactions to give often quite complex morphologies in a process that is closely related to crystallization.[12] In some cases it is thought that the solid-state structure of the gel fibers is the same as the structure of the crystalline gelator.[13,14] However, more commonly, either a different structure is adopted or the structure is unknown because the poorly crystalline nature of the gel or dried gel (xerogel) does not give powder X-ray diffraction (PXRD) patterns that are amenable to structure solution and refinement by Rietveld methods. The most common classes of gelators include nucleobases, saccharides, peptides, ureas,[15,16] and steroid derivatives.[12] Nucleobases[17,18] and related planar components, such as melamine[19,20] in particular, are interesting because of the multiple hydrogen-bonding interactions between complementary nucleobase pairs, suggesting that robust supramolecular gels might arise. In general however, nucleobases and other related heterocycles must be derivatized with long alkyl chains to give appropriate solubility properties and allow extensive hydrophobic interactions before they can act as gelators. Underivatized, rigid, planar molecules with such good hydrogen bonding functionality are commonly very insoluble as a result of the formation of very stable π-stacking and infinite hydrogen bonded chains in the solid state. Recent reports have shown, however, that sonication can induce gel formation.[21,22] Sonication is more commonly used to increase the dissolution rate of insoluble compounds. We reasoned that there may be a link between sonication-induced gelation and the partial solubilization of insoluble compounds, particularly for those compounds with strong hydrogen bonding functionality. Sonication-induced dissolution of small quantities of strongly hydrogen-bonding species may result in their rapid aggregation under nonequilibrium conditions and the deposition of a fibrous material without time for full crystallization to take place. Herein we present hydrogelation by a mixed system comprising two entirely rigid, insoluble, mutually complementary, planar multifunctional hydrogen-bond donor/acceptors, namely melamine and uric acid (denoted M and U; Scheme 1), and we propose the likely structure of the gel from the results of crystal structure prediction calculations.[23–25]

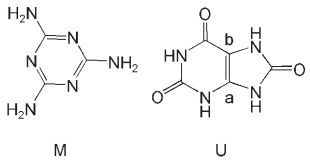

Scheme 1. Structures of melamine (M, left) and uric acid (U, right). Bridgehead atoms C_a and C_b of uric acid are labeled.

The melamine–uric acid (M–U) pair is related to the well-known melamine–cyanuric acid rosette assemblies;[26,27] however, uric acid was chosen because of the donor–donor–acceptor arrangement (DDA as opposed to ADA) of one face, which we felt might lower the crystallinity of any resulting assembly. Uric acid and in particular melamine are both only very sparingly soluble in cold water, and mixing melamine and uric acid in a 1:1 ratio in cold water does not result in any observable reaction or dissolution. However, repeated sonication and shaking of a 1:1 mixture in distilled water at room temperature results in gelation over a period of about five minutes at concentrations of 0.8 weight percent or greater. If lower concentrations are used, a partial gel forms. Warming or shaking the sample results in a viscous liquid that gels upon standing. This process is speeded up markedly upon sonication for about ten seconds. Gelation may be reinduced by sonication. The resulting gel was dried in an oven at 85 °C and characterized by scanning electron microscopy (SEM) which showed a dense, well-defined network of collinear

[*] Dr. K. M. Anderson, P. Byrne, Dr. N. Clarke, Prof. J. W. Steed
Department of Chemistry, Durham University
South Road, Durham, DH1 3LE (UK)
Fax: (+44) 191-384-4737
E-mail: jon.steed@durham.ac.uk
Dr. G. M. Day
Department of Chemistry, University of Cambridge
Lensfield Road, Cambridge, CB2 1EW (UK)
Dr. M. J. Paterson
Department of Chemistry, School of Engineering and Physical Sciences, Heriot-Watt University
Edinburgh, EH14 4AS (UK)

[**] We thank the EPSRC for funding (grants EP/E023339/1 and EP/E031153/1) and Dr. D. C. Apperley and Mr. A. F. Markwell for help with the MAS-NMR spectroscopic data. G.M.D. thanks the Royal Society for a University Research Fellowship.

Supporting information for this article is available on the WWW under http://www.angewandte.org or from the author.

fibers, each circa 30 nm wide (Figure 1a), which is typical of gels.[12] Cryoscopic SEM images were also obtained by flash freezing the undried gel and then warming under vacuum to evaporate water. The result (Figure 1b) was a much less dense network that is possibly more representative of the fiber

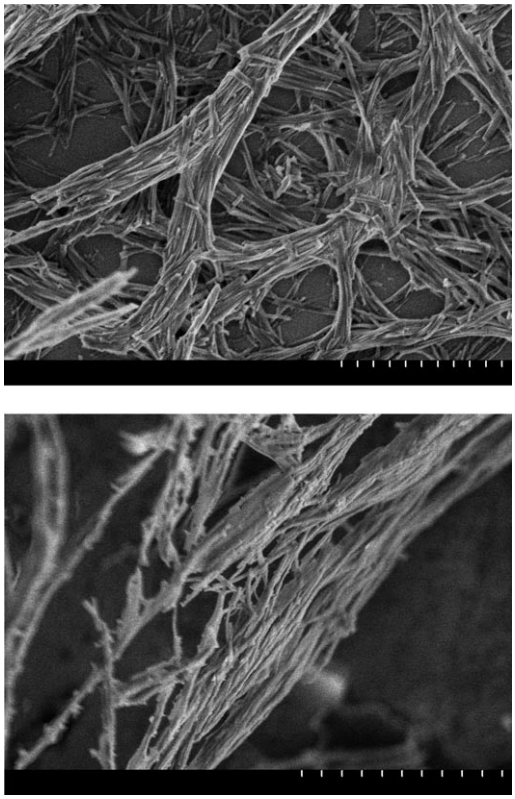

Figure 1. SEM images of the M–U gel. Above: xerogel, and below: frozen gel slowly warmed under vacuum to evaporate water (each division corresponds to 200 nm on the scale bars).

density in the gel before the surface-tension-induced collapse caused by drying and suggesting that the gel nanostructure is quite robust. Repeated frequency-sweep rheometry measurements of the gel confirmed that the storage modulus G' is significantly higher than the loss modulus G'', and is invariant with frequency up to up to a yield point of about 125 Hz, confirming the characteristic viscoelasticity of the gels.[12] Elemental analysis of the xerogel suggests a dihydrate of formula M·U·2 H_2O, and the presence of water was confirmed by thermal gravimetric analysis, which showed very gradual water loss up until 316 °C followed by sudden decomposition. Interestingly, this temperature is significantly above the decomposition temperature of pure melamine (280 °C), suggesting that the melamine is significantly stabilized in the gel phase. In confirmation, gel samples enriched with excess melamine showed melamine loss at this temperature before the decomposition of the gel phase itself. Variation of the gel composition from M–U ratios of 9:1 through 1:1 to 1:9 and measurement of the rheology of the resulting gels gave a distinct maximum in plateau elastic modulus and yield stress at 1:1 ratio, confirming the 1:1 composition of the gels (see Supporting Information).

Further evidence for the formation of a distinct M·U·2 H_2O phase was obtained from ^{13}C MAS-NMR spectroscopy of the xerogel, which revealed the presence of both components M and U with significant chemical shift changes, particularly for the signal corresponding to bridgehead carbon C_a (Scheme 1), which changes in position from $\delta =$ 138 ppm in free uric acid to $\delta = 144$ ppm in the xerogel. The xerogel also exhibits a much shorter relaxation time compared to both the free components. In contrast, solid-state grinding of melamine and uric acid under atmospheric conditions (but without added water) results in a material displaying a ^{13}C MAS-NMR spectrum that is a superposition of the spectra for the two pure components and having a characteristically long relaxation time. Similarly, the PXRD pattern of the ground mixture is a superposition of those of the pure components, thus the xerogel phase cannot be obtained mechanochemically, highlighting the importance of sonication in its formation.[28]

The PXRD pattern for the dried xerogel is shown in Figure 2d. The broadness of the peaks and lack of diffraction beyond about 40° in 2θ (Cu radiation) suggests that the material is not particularly crystalline, as might be expected; however the close spacing of the low-angle peaks implies a large unit cell, consistent with the three different hydrogen bonding faces of the unsymmetrical uric acid molecule. The very pronounced peak at 27.7° corresponds to a d spacing of 3.2 Å, and is very close to typical π–π stacking interactions in the single crystal structures of melamine–cyanuric acid[26] and bis(melaminediium)melamine tetrachloride hexahydrate[29]

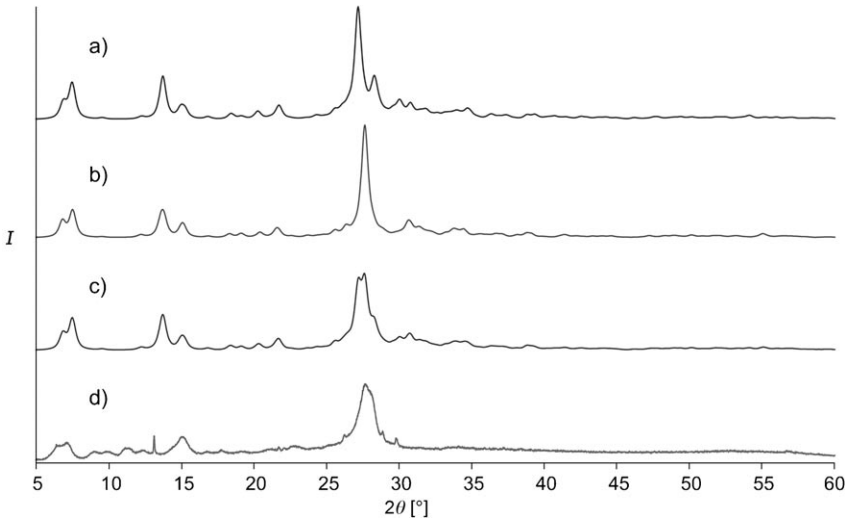

Figure 2. Comparison of the simulated PXRD patterns from a) the predicted fourth-lowest-energy M·U·2 H_2O structure, b) the calculated higher-energy structure, c) the average PXRD pattern from the two calculated structures, and d) the experimental xerogel PXRD pattern.

of 3.20 and 3.25 Å, respectively. Essentially identical PXRD patterns were obtained, irrespective of gelator concentration and drying method.

To understand the structure of the gel, MP2/aug-cc-pVDZ calculations were undertaken on four possible hydrogen-bonded M–U pairs. The MP2-minimized structures of the four possibilities are shown in Figure 3 a–d. The primary amine

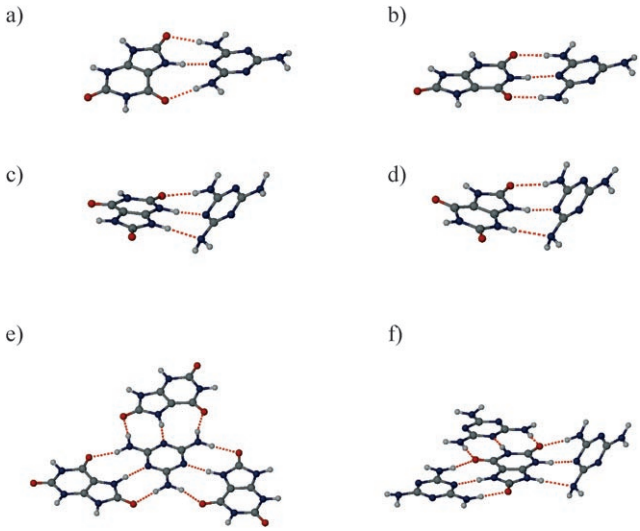

Figure 3. a–d) MP2-minimized structures of hydrogen-bonded M–U pairs: a) coplanar ADA···DAD type, $\Delta E = 0.82$ kJ mol^{-1}, b) coplanar ADA···DAD type, $\Delta E = 7.17$ kJ mol^{-1}, c) noncoplanar ADD···DAA type, $\Delta E = 0$ kJ mol^{-1} and d) noncoplanar ADD···DAA type, $\Delta E = 3.51$ kJ mol^{-1}. e and f) DFT(PBE1PBE/6-31 + G*)-minimized structures of hydrogen bonded M–U quartets M–U_3 (e) and M_3–U (f).

nitrogen atoms of melamine exhibit significant pyramidalization (consistent with the neutron structure of melamine[30]), allowing them to act as hydrogen bond acceptors to give two nonplanar pairs of type AAD···DDA, shown in Figure 3 c, d, as well as two ADA···DAD planar pairs (Figure 3 a, b), as found in melamine–cyanuric acid.[26,27] Both of these nonplanar geometries occur on the wide DDA face of uric acid, centered on atom C_a. All four pairs shown in Figure 3 a–d have similar energies, with one of the noncoplanar interactions having the lowest energy as a result of fewer unfavorable diagonal H···H repulsions.[31] Using these interactions, we then built up two quartet models as a guide to the possible environment of typical uric acid and melamine molecules surrounded by three of the complementary partner. The quartet models were studied by DFT (PBE1PBE/6-31 + G*). Although it is possible to surround melamine with three uric acid molecules in a coplanar fashion (Figure 3 e), the uric acid molecule must involve one of the noncoplanar interactions on its wide face (Figure 3 f).

This noncoplanar arrangement will tend to reduce the stabilization arising from π–π stacking interactions, and hence may be an explanation for the inclusion of water molecules within the lattice. To explore the low energy crystal packing possibilities, we attempted to calculate likely crystal structures for the M–U complex both in the absence of water and as a dihydrate, M·U·2 H_2O (as suggested by analytical and TGA data), using methods developed for small molecule ab initio crystal structure prediction.[23–25] The resulting low-energy computer-generated crystal structures should give insight into the most stable packing possibilities and patterns of intermolecular interactions in this system and, in combination with the available experimental observations, could provide a likely structure for the gel. Although such calculations have only rarely been applied to multicomponent cocrystals (and never, to our knowledge, for three-component crystals), recent studies have shown their promise for predicting and understanding the crystallization behavior of solvates and cocrystals.[32,33]

Putative crystal structures were generated using a quasi-random sampling of unit cell dimensions, molecular positions, and orientations of the two (for M·U) or four (for M·U·2 H_2O) independent molecules in the most commonly observed space groups for molecular organic crystals. The best structures were then energy-minimized using a high-quality model intermolecular potential, with atomic multipole electrostatics, and allowing flexibility around the melamine primary amine nitrogen atoms in a manner recently proposed for crystal structure prediction of flexible molecules.[34] (Details of the methods are provided in the Supporting Information.) Both sets (M·U and M·U·2 H_2O) of computer-generated crystal structures were then analyzed for preferred patterns of intermolecular interactions, to see which of the M–U pairs from the MP2 study are present in well-packed crystal structures (see the Supporting Information). Furthermore, powder X-ray diffraction patterns were calculated for all low-energy structures for comparison with the diffraction pattern measured from the xerogel. For the anhydrous structures, the most common dimer in the low-energy crystal structures is the lower-energy coplanar ADA···DAD pair (Figure 3 a), which is found in about two-thirds of the low-energy structures (Supporting Information, Figure S1a). Almost all remaining structures contain the higher-energy coplanar dimer (Figure 3 b), and the two coplanar M–U pairings rarely combine in the same structure. The noncoplanar ADD···DAA hydrogen-bond pairs are rarely found in the low-energy crystal structures; the high-energy noncoplanar pair (Figure 3 d) is not present in any of the structures, although the low-energy noncoplanar M–U pair (Figure 3 c) is sometimes found in combination with one of the coplanar pairs. PXRD patterns were simulated from all of the low-energy anhydrous structures, but none matched the observed PXRD data from the dried xerogel (Supporting Information, Figure S7).

Calculations on the dihydrate M·U·2 H_2O proved much more challenging—to our knowledge, crystal structure prediction has never before been attempted with four independent molecules in the asymmetric unit ($Z'' = 4$), and the process required the minimization of circa 270 000 candidate structures. As in the anhydrous structures, most of the low-energy possibilities contain the coplanar ADA···DAD hydrogen bond pairs. However, unlike with the predictions for the anhydrous structures, the combination of both planar dimer interactions (Figure 3 a, b) is quite common in the calculated dihydrate crystal structures (Supporting Information,

Figure S1b). The water molecules frequently interact with the DDA face of uric acid, in preference to noncoplanar M–U pairs, which do not occur in any of the calculated structures.

We also noted the difference in lattice energy between the best M·U and M·U·2 H_2O crystal structures: the lowest energy M·U crystal structure has a calculated lattice energy of about $-298\ kJ\,mol^{-1}$, whereas the lattice energy of the best dihydrate structure is $-396\ kJ\,mol^{-1}$. The gain in energy on forming the dihydrate instead of a pure M–U phase outweighs the energetic cost of removing two water molecules from bulk water ($2\times\Delta H_{vap,water}=81\ kJ\,mol^{-1}$), so the calculations support the thermodynamic preference of a dihydrate structure over pure melamine–uric acid.

Simulated PXRD patterns from the computer-generated crystal structures were compared to that observed from the dried xerogel both visually and using de Gelder's normalized weighted cross-correlation similarity function.[35] We found a very good match with the observed PXRD pattern from the calculated fourth-lowest-energy structure (Figure 2a), which gave a similarity measure of 0.9524 over the 2θ range 2–60° using a fixed-full-width at half-maximum of 0.1° 2θ when simulating the pattern. This is the highest similarity measure obtained from the structures within 10 $kJ\,mol^{-1}$ of the lowest-energy calculated structure, and the similarity measure increases to 0.9650 using a fixed-full-width at half-maximum of 0.5° 2θ, which is more representative of the peak broadness in the observed pattern. We also identified a very similar higher energy structure that also gave a good match to the observed PXRD pattern (Figure 2b). The two calculated structures (indicated in Supporting Information, Figure S1b) differ only by slight changes in the water molecule positions and geometry of the melamine amines, leading to a slight change in the position of the strong peak in the PXRD pattern near 28°. Averaging the two calculated patterns improves the match still further (Figure 2c). The observations suggest that these structures provide the likely melamine–uric acid framework of the gel structure, and disorder in the water positions leads to the broadness of the observed PXRD peak at 27.7°. We thus conclude that it is possible to use crystal structure prediction to give meaningful information about xerogel and hence gel structure. The predicted structure that matches the experimental results contains U–U pairwise interactions as well as the two coplanar M–U pairs, and the water molecules are aligned in channels, interacting with the remaining U and M faces (Figure 4). The unit cell is highly anisotropic and exhibits sheets of strong hydrogen bonding interactions. This 2D anisotropy may contribute to the tendency of the material to form gels with a tapelike morphology, as seen in Figure 1a.

In conclusion, we have shown that a robust hydrogel arises from the cocrystallisation of two mutually complementary rigid components and water. The DDA face of the uric acid favors incorporation of water molecules into the crystalline lattice. Despite the resulting complexity of the structure, it is possible to use crystal-structure prediction methods to calculate a reliable model for the structure of the xerogel that is consistent with experimental data from a variety of different techniques. This work highlights the similarities between gelation and crystallization processes, and opens a new avenue for the understanding and control of gel structure and ultimately properties using methods derived from the study of fully crystalline materials.

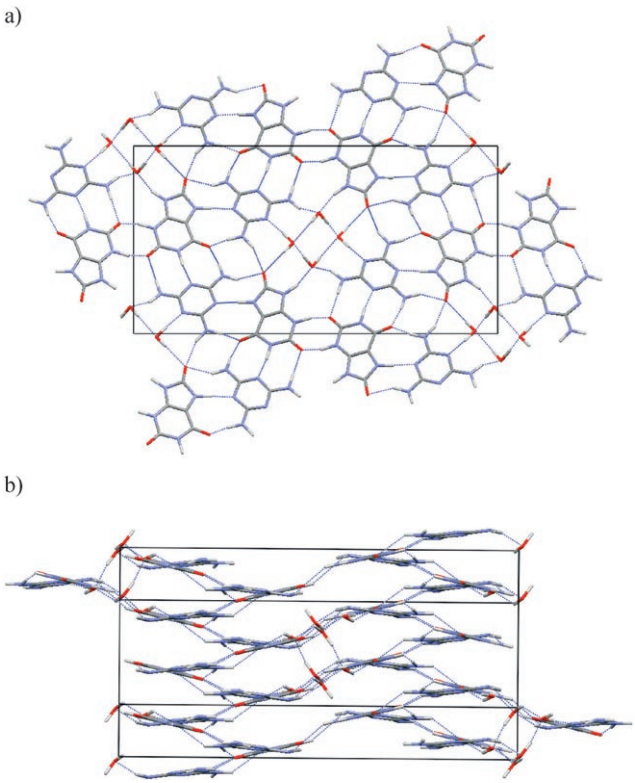

Figure 4. Calculated fourth-lowest-energy crystal structure of M·U·2 H_2O; monoclinic, $P2_1/c$, $a=3.818$, $b=25.810$, $c=14.088$ Å, $\beta=71.17°$. a) View down the *a* axis, and b) view side-on to the hydrogen bonding.

Received: August 17, 2007
Revised: November 9, 2007
Published online: December 28, 2007

Keywords: crystal engineering · gels · hydrogen bonds · sonication · structure elucidation

[1] L. A. Estroff, A. D. Hamilton, *Chem. Rev.* **2004**, *104*, 1201.
[2] R. G. Ellis-Behnke, Y. X. Liang, S. W. You, D. K. C. Tay, S. G. Zhang, K. F. So, G. E. Schneider, *Proc. Natl. Acad. Sci. USA* **2006**, *103*, 5054.
[3] K. Y. Lee, D. J. Mooney, *Chem. Rev.* **2001**, *101*, 1869.
[4] A. Friggeri, B. L. Feringa, J. van Esch, *J. Controlled Release* **2004**, *97*, 241.
[5] J. C. Tiller, *Angew. Chem.* **2003**, *115*, 3180; *Angew. Chem. Int. Ed.* **2003**, *42*, 3072.
[6] C. S. Love, V. Chechik, D. K. Smith, K. Wilson, I. Ashworth, C. Brennan, *Chem. Commun.* **2005**, 1971.
[7] P. K. Vemula, G. John, *Chem. Commun.* **2006**, 2218.
[8] Q. Wei, S. L. James, *Chem. Commun.* **2005**, 1555.
[9] S. Kiyonaka, K. Sugiyasu, S. Shinkai, I. Hamachi, *J. Am. Chem. Soc.* **2002**, *124*, 10954.
[10] F. Fages, *Angew. Chem.* **2006**, *118*, 1710; *Angew. Chem. Int. Ed.* **2006**, *45*, 1680.
[11] L. Applegarth, N. Clark, A. C. Richardson, A. D. M. Parker, I. Radosavljevic-Evans, A. E. Goeta, J. A. K. Howard, J. W. Steed, *Chem. Commun.* **2005**, 5423.

[12] P. Terech, R. G. Weiss, *Chem. Rev.* **1997**, *97*, 3133.
[13] D. J. Abdallah, R. G. Weiss, *Adv. Mater.* **2000**, *12*, 1237.
[14] D. R. Trivedi, P. Dastidar, *Chem. Mater.* **2006**, *18*, 1470.
[15] C. E. Stanley, N. Clarke, K. M. Anderson, J. P. Lenthall, J. W. Steed, *Chem. Commun.* **2006**, 3199.
[16] M. de Loos, B. L. Feringa, J. H. van Esch, *Eur. J. Org. Chem.* **2005**, 3615.
[17] K. Araki, I. Yoshikawa, *Top. Curr. Chem.* **2005**, *256*, 133.
[18] A. Ghoussoub, J.-M. Lehn, *Chem. Commun.* **2005**, 5763.
[19] K. Hanabusa, T. Miki, Y. Taguchi, T. Koyama, H. Shirai, *J. Chem. Soc. Chem. Commun.* **1993**, 1382.
[20] S. Manna, A. Saha, A. K. Nandi, *Chem. Commun.* **2006**, 4285.
[21] T. Naota, H. Koori, *J. Am. Chem. Soc.* **2005**, *127*, 9324.
[22] Y. Li, T. Wang, M. Liu, *Tetrahedron* **2007**, *63*, 7468.
[23] G. M. Day, W. D. S. Motherwell, W. Jones, *Phys. Chem. Chem. Phys.* **2007**, *9*, 1693.
[24] A. J. Cruz Cabeza, G. M. Day, W. D. S. Motherwell, W. Jones, *J. Am. Chem. Soc.* **2006**, *128*, 14466.
[25] G. M. Day, W. D. S. Motherwell, H. L. Ammon, S. X. M. Boerrigter, R. G. Della Valle, E. Venuti, A. Dzyabchenko, J. D. Dunitz, B. Schweizer, B. P. van Eijck, P. Erk, J. C. Facelli, V. E. Bazterra, M. B. Ferraro, D. W. M. Hofmann, F. J. J. Leusen, C. Liang, C. C. Pantelides, P. G. Karamertzanis, S. L. Price, T. C. Lewis, H. Nowell, A. Torrisi, H. A. Scheraga, Y. A. Arnautova, M. U. Schmidt, P. Verwer, *Acta Crystallogr. Sect. B* **2005**, *61*, 511.
[26] A. Ranganathan, V. R. Pedireddi, C. N. R. Rao, *J. Am. Chem. Soc.* **1999**, *121*, 1752.
[27] G. M. Whitesides, E. E. Simanek, J. P. Mathias, C. T. Seto, D. N. Chin, M. Mammen, D. M. Gordon, *Acc. Chem. Res.* **1995**, *28*, 37.
[28] A. L. Garay, A. Pichon, S. L. James, *Chem. Soc. Rev.* **2007**, *36*, 846.
[29] A. Ishii, S. Kishi, K. Maeda, H. Ichikawa, K. Mizuoka, Y. Ikeda, M. Hasegawa, private communication to the CSD, refcode VECTAZ, **2005**.
[30] A. Cousson, B. Nicolaï, F. Fillaux, *Acta Crystallogr. Sect. E* **2005**, *61*, o222.
[31] G. A. Jeffrey, *An Introduction to Hydrogen Bonding*, 1st ed., OUP, Oxford, **1997**.
[32] A. T. Hulme, S. L. Price, *J. Chem. Theory Comput.* **2007**, *3*, 1597.
[33] A. J. Cruz Cabeza, G. M. Day, W. D. S. Motherwell, W. Jones, *J. Am. Chem. Soc.* **2006**, *128*, 14466.
[34] G. M. Day, W. D. S. Motherwell, W. Jones, *Phys. Chem. Chem. Phys.* **2007**, *9*, 1693.
[35] R. de Gelder, R. Wehrens, J. A. Hageman, *J. Comput. Chem.* **2001**, *22*, 273.

